# Light-Harvesting Mechanism of Bacteria Exploits a Critical Interplay between the Dynamics of Transport and Trapping

Felipe Caycedo-Soler, Ferney J. Rodríguez, and Luis Quiroga
*Departamento de Física, Universidad de Los Andes, A.A. 4976 Bogotá, Colombia*

Neil F. Johnson
*Department of Physics, University of Miami, Coral Gables, Miami, Florida 33126, USA*
(Received 24 June 2009; published 16 April 2010)

Light-harvesting bacteria *Rhodospirillum photometricum* were recently found to adopt strikingly different architectures depending on illumination conditions. We present analytic and numerical calculations which explain this observation by quantifying a dynamical interplay between excitation transfer kinetics and reaction center cycling. High light-intensity membranes exploit dissipation as a photoprotective mechanism, thereby safeguarding a steady supply of chemical energy, while low light-intensity membranes efficiently process unused illumination intensity by channeling it to open reaction centers. More generally, our analysis elucidates and quantifies the trade-offs in natural network design for solar energy conversion.

DOI: 10.1103/PhysRevLett.104.158302 PACS numbers: 82.37.Rs, 81.16.Pr, 87.15.A−, 87.15.hj

Photosynthesis is nature's solution to the solar energy conversion problem [1–5]. Understanding what architectural designs it adopts, and why, are important questions which could guide designs of future energy conversion devices. Many studies have clarified the exciton capture-transfer dynamics of reaction center (RC) pigment-protein complexes [4–9], their arrangement along the membranes that support them [10–15], and even RC quantum effects [16,17]. Recent experimental investigations [10] resolved the locations of light-harvesting (LH) complexes within the 2D membrane architecture of complete chromatophore vesicles, to reveal an unexpected change in the ratio of complexes for bacteria grown under high [Fig. 1(a)] versus low illumination intensities [Fig. 1(b)].

This Letter presents analytic and numerical results which explain this experimental observation [10] by quantifying a trade-off which arises between two fundamental membrane requirements: (1) the need to convert large numbers of excitations into energetically useful charge separations within the RC, and hence promote metabolic activity, and (2) the need to avoid an oversupply of excitations and hence excessive bursts of energy, which could damage the photosynthetic machinery [10,11]. Within our theory, the microscopic origin of this trade-off is the interplay between excitation transfer kinetics across the membrane architecture and reaction center cycling dynamics. This generates a critical behavior of the membrane's efficiency when probed under different light intensities. Low light-intensity membranes (LLIMs) efficiently channel excess illumination intensity to open reaction centers, and hence are dominated by (1), while high light-intensity membranes (HLIMs) better exploit excitation loss through dissipation as a photoprotective mechanism in order to provide constant chemical energy, and hence are dominated by (2). Our analytic model predicts a critical light intensity during growth, below which the synthesis of LH2 complexes should be dramatically enhanced.

The photosynthesis process in purple bacteria [4,5] [see Fig. 1(c)] involves photons from sunlight being absorbed

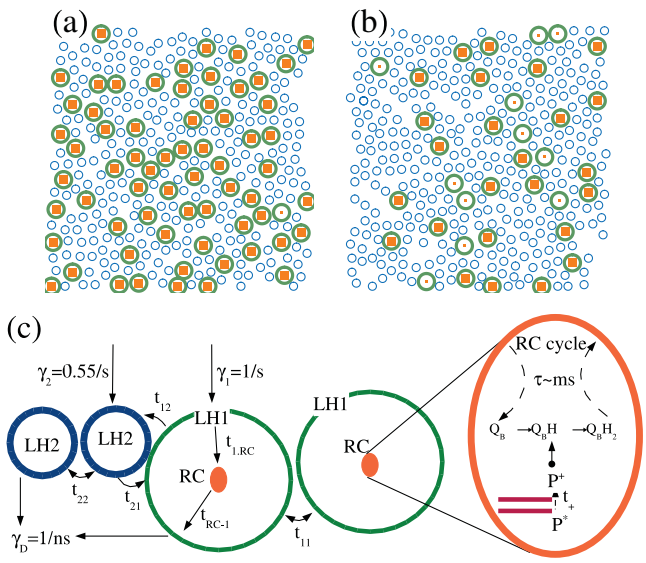


FIG. 1 (color). Top panels: Empirical architectures (i.e., digitized positions of LH complexes) from Ref. [10]. (a) High light-intensity membrane (HLIM), $I_0 = 100$ W/m$^2$. (b) Low light-intensity membrane (LLIM), $I_0 = 10$ W/m$^2$. Small orange dots: open reaction centers (RC) at snapshot during simulation. Large orange boxes: closed RCs. Large green circles: LH1s. Small blue circles: LH2s. (c) Summary of dynamical processes of excitation transfer between LH1-LH1, LH2-LH2, LH1-LH2, LH1-RC. Dissipation ($\gamma_D$), absorption ($\gamma_{1(2)}$) and RC cycling time $\tau$ (enlarged orange oval) are also shown.

 

with a rate $\gamma_A = I(\gamma_1 N_1 + \gamma_2 N_2)$, where $N_{1(2)}$ is the number of LH1 (LH2) complexes, $\gamma_{1(2)}$ [3] are the respective absorption rates per complex, and $I$ is the light intensity. Each LH1 contains one RC; i.e., the number of RCs is equal to $N_1$. Excitation transfer between light-harvesting complexes occurs at the following mean times (picoseconds) [8,9,17]: $t_{12} = 15$ for LH1-LH2; $t_{21} = 3.3$ for LH2-LH1; $t_{11} = 20$ for LH1-LH1; $t_{22} = 10$ for LH2-LH2; before reaching an RC at time $t_{1,\mathrm{RC}} = 25$ for LH1-RC. Once in an open RC, the special pair may become ionized ($P^+$) on the time scale $t_+ = 3$, eventually producing quinol ($Q_B H_2$) by reducing quinone ($Q_B \rightarrow Q_B^- \rightarrow Q_B H$) twice [1]. Otherwise back transfer occurs from RC to LH1 with $t_{\mathrm{RC},1} = 8$. Before a new $Q_B$ becomes available, the RC remains closed for a cycling time $\tau$ during which an energetically useful charge separation is generated [3,11,18,19]. Dissipation through fluorescence or internal conversion happens at a constant rate $\gamma_D$ [3]. The photoexcitation kinetics can be described by a collective population state vector $\rho(t)$ which follows a master equation $\partial_t \rho_i(t) = \sum_j G_{ij}\rho_j(t)$, where the element $G_{ij}$ of the rate matrix establishes the probability per unit time of a transition (due to absorption, dissipation, RC ionization, transfer to neighbors) between collective states $i$ and $j$. Because of small absorption rates, the probability that two excitations occupy either a single harvesting structure or RC is negligible. Light-harvesting complexes only have two possible states: no exciton present (unexcited) or one exciton state (excited). However, the RC has four possible states: (un)excited while being open or closed. Hence the state space has size $2^{N_1}2^{N_2}4^{N_1} = 2^{3N_1+N_2}$.

Vesicles imaged with experimental atomic force microscopy (AFM) [10] show that typically $2N_1 + N_2 \approx$ 300–600. Given the large state space, we study a discrete-time random walk simulation for excitations which includes dynamical coupling to open or closed RC states, in contrast to Refs. [4,8]. We use the empirical architectures [10] to establish the likely neighbors (e.g., within 30 Å) between which excitations can hop, and implement the process of absorption and excitation transfer, dissipation, or RC capture (if within a RC) using Monte Carlo numerical simulations. All processes obey exponential distributions with mean values presented in Fig. 1(c). When two excitations reach a single RC, it closes for the cycling time $\tau$ [3,11,18,19]. We checked the accuracy of our stochastic numerical simulation by comparing its population-level predictions to those of a master equation for small chromatophores [20]. The HLIM and LLIM architectures (Fig. 1, top panel) differ in the relative number of complexes and have stoichiometry $s = N_2/N_1$. A typical snapshot of open and closed RCs from our stochastic simulations [see Fig. 1(a) and 1(b)] demonstrates that HLIM has fewer open RCs than LLIM in the experimentally relevant regime of millisecond RC-cycling times [18,19]. Our interest is the actual quinol output of the membrane; hence, we calculate stationary-state observables when the numerical simulations converge to a constant quinol rate. The quinol production rate $W = \frac{1}{2}\frac{dn_{\mathrm{RC}}}{dt}$ is half the rate at which $n_{\mathrm{RC}}$ excitations produce ionization $P^+$. Assuming similar metabolic requirements under different illumination growth, the times suggested by arrows in Fig. 2(a) imply that LLIM has a shorter RC-cycling time than HLIM. This is consistent with greater quinone availability in LH1 clusters, as appropriate in LLIMs [11].

We find qualitatively different behaviors in $W$ as a function of normalized intensity $I/I_0$ [see Fig. 2(a) inset]. In HLIM, greater intensity does not change the quinol rate, while in LLIM higher illumination increases $W$. Therefore for higher light intensity, LLIM will be better than HLIM at processing potentially dangerous occurrences of excess excitations. Because of fewer open RCs, HLIM will process only the necessary number of excitations for metabolism. The efficiency $\eta = n_{\mathrm{RC}}/n_A$ is related to the quinol rate in the stationary limit through $\eta = 2W/\gamma_A$, and quantifies the performance of a membrane in initiating RC ionizations from the $n_A$ total absorbed excitations. Figure 2(b) shows that increased light intensity lowers $\eta$ in both membranes due to a reduced number of open RCs ($N_0$), as shown by the distributions $p(N_o)$ of open RCs at the top of Fig. 2(b). Consequently LLIMs have better efficiency than HLIMs since they have more open RCs in the high light-intensity range, even though they have fewer RCs.

An intriguing question arises as to whether clustering of LH1s might help reduce the effective path that an excita-

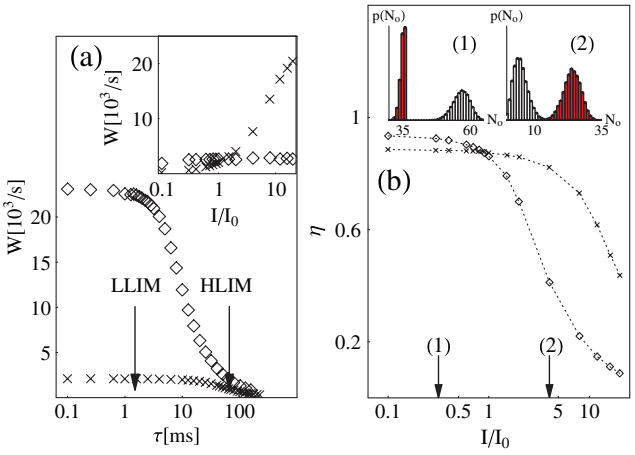


FIG. 2 (color). (a) $W(\tau)$ for LLIM (crosses) and HLIM (diamonds). The inset shows the quinol rate with respective RC-cycling times for which LLIM has the same quinol output as HLIM, shown with arrows in the main plot. (b) Efficiency $\eta$ as a function of normalized intensity $I/I_0$ for $\tau = 3$ ms in HLIM (diamonds) and LLIM (crosses) adapted membranes. Dotted lines are aids to the eye. In insets, distribution of open RCs, $p(N_o)$, in HLIM (white bars) and LLIM (red bars) adapted membranes, are shown for the values highlighted by arrows in main plots. Error bars smaller than the symbols are not shown.

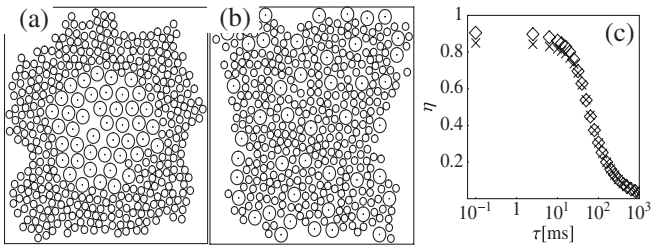


FIG. 3. (a) Ordered and (b) random membranes with $s = 8.09$. (c) presents $\eta(\tau)$ for ordered (crosses) and random (diamonds) membranes.

tion needs to take to a closed RC [10]. To explore this, we consider two extreme chromatophore vesicles [Figs. 3(a) and 3(b)], both of which are compatible with relevant LLIM stoichiometries [14]. Their efficiencies are shown in Fig. 3(c). In the experimentally relevant regime of millisecond RC-cycling time, open RCs are sparse—they are not clustered, and the architecture has no significant influence on $\eta$. Less clustering does induce a slightly higher efficiency since the RC borders become easier to reach [8,20]. However, apart from the benefit of quinone exclusion, clustering seems not to appreciably diminish the path length of excitations reaching a closed RC. On the other hand, clustering of LH2s might exclude active quinones from LH1-RC domains, thereby increasing their availability in core clusters and decreasing the RC-cycling time. Efficiency of the membranes will also depend on $\tau$, since this dictates how fast an RC opens due to a new quinone being available. If $\tau$ is taken as a parameter, very small differences appear between membranes having equal stoichiometries but different network architectures. In Fig. 4(a), we compare the efficiencies of the representative architectures presented in Fig. 1, calculated using the numerical stochastic simulations, as a function of RC-cycling time. In their respective illumination regimes, LLIM dissipates fewer excitations for $\tau$ values in the biologically relevant millisecond range [18,19]. This implies that even if their RC-cycling times are equal (i.e., no enhanced quinone diffusion in clustered LLIM), LLIM is efficient ($\eta \approx 85\%$) while HLIM provides a steady quinol supply by exploiting dissipation ($\eta \approx 20\%$–$40\%$). These findings hold irrespective of any other diffusion enhancements.

Guided by these numerical findings, we now develop an analytic model to capture the underlying physics. Assume that $N_E$ excitations are created in the membrane at an absorption rate $\gamma_A$. Excitations either leave the membrane through dissipation at a rate $\gamma_D$, or at an RC at rate $\lambda_C$ where $\lambda_C$ depends on $N_o$. The number of RCs closing per unit of time is $\lambda_C N_E/2$, while the number opening per unit of time is $\frac{1}{\tau}(N_1 - N_o)$. Hence the number of absorbed photons is connected to the number of available (open) RCs by the following pair of coupled differential equations:

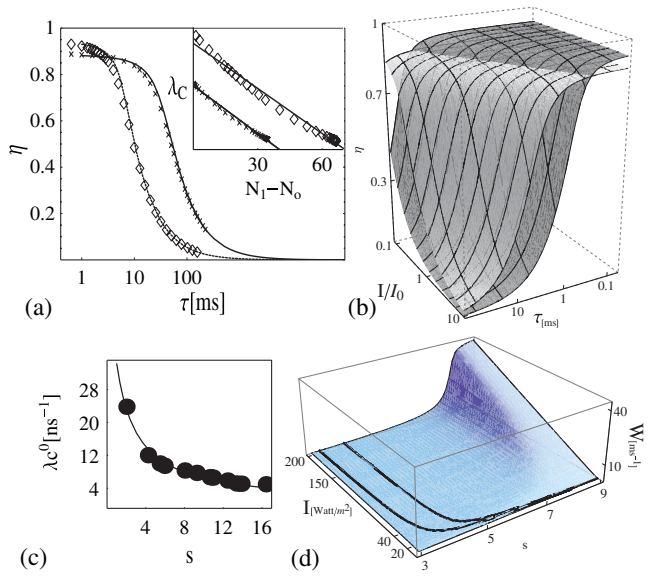


FIG. 4 (color). (a) Analytical model (continuous) and stochastic simulation (HLIM: diamonds, LLIM: crosses). Inset: $\lambda_C(N_o)$ from Monte Carlo simulations. Parameter values for LLIM and HLIM are $\lambda_C^0 = \{0.00771, 0.0163\}$ ps$^{-1}$ and $N_1 = \{40.01, 70.66\}$ respectively, consistent with empirical values. (b) $\eta$, as function of $\tau$ and $I/I_0$, obtained from complete analytical solution for LLIM (white) and HLIM (gray). (c) Numerical calculation of $\lambda_C^0(s)$ (dots) vs our analytic form from text (continuous). (d) $W(s, I)$ as function of stoichiometry $s$ and illumination intensity, with quinol rate contours of 1900 and 2100 s$^{-1}$.

$$\frac{dN_E}{dt} = -[\lambda_C(N_o) + \gamma_D]N_E + \gamma_A, \tag{1}$$

$$\frac{dN_o}{dt} = \frac{1}{\tau}(N_1 - N_o) - \frac{1}{2}\lambda_C(N_o)N_E. \tag{2}$$

When $\lambda_C = 0$, all RCs are closed. The maximum value ($\lambda_C^0$) occurs when all RCs are open. When the membrane is excited, the transfer-ionization rate per open RC is constant due to the fast excitation hopping relative to the cycling time, i.e., $\lambda_C/N_o = \lambda_C^0/N_1$ which is also supported by numerical simulations [see Fig. 4(a) inset]. Given that $\eta = \lambda_C^0 N_o N_E/(N_1\gamma_A)$, the steady state solution to Eqs. (1) and (2) is [20]:

$$\eta = \frac{1}{2\gamma_A\lambda_C^0\tau}\{2N_1(\lambda_C^0 + \gamma_D) + \gamma_A\lambda_C^0\tau - [4N_1^2(\lambda_C^0 + \gamma_D)^2 + 4N_1\gamma_A\lambda_C^0(\gamma_D - \lambda_C^0)\tau + (\gamma_A\lambda_C^0\tau)^2]^{1/2}\}. \tag{3}$$

In the limit of fast RC-cycling time ($\tau \to 0$), $\eta$ has the simple form $\eta = (1 + \gamma_D/\lambda_C^0)^{-1}$. If all transfer paths are summarized by $\lambda_C^0$, this solution illustrates that $\eta \geq 0.9$ [8], if the transfer-$P$ reduction time is less than one tenth of the dissipation time in the absence of RC cycling. For finite $\tau$ this analytic solution is in very good quantitative agreement with the numerical stochastic simulation, supporting

our previously discussed interpretation [see Fig. 4(a)]. Figure 4(b) shows the complete analytical solution of Eqs. (1) and (2), in order to confirm the entire range of light intensities and RC closing times for which LLIM has a higher efficiency than HLIM. The assumed linear fit for $\lambda_C$ smears out an apparent power-law behavior. We have yet to find analytical solutions for $\eta$ in cases where $\lambda_C(N_o)$ has a power-law dependence.

Our analytical model can be used for easy comparison of the metabolic outputs from experimentally distinct AFM-imaged membranes, in order to provide additional insight concerning the adopted and expected stoichiometries in *Rhodospirillum photometricum* [10]. The bacteria are studied under different illumination conditions, assuming that comparable metabolic needs (i.e., quinol supply) are accomplished in vesicles of area $A_0$. Our present aim is to find an expression for the quinol production rate $W$ in terms of the environmental growth conditions and the responsiveness of purple bacteria through stoichiometry adaptation. In the stationary state, $W = \lambda_C N_E/2$ depends on the number of excitations within the membrane and on the details of transfer through the rate $\lambda_C$. The LH1 and LH2 complexes of area $A_1$ and $A_2$, respectively, fill a fraction $p$ of the total vesicle area $p = (A_1 N_1 + A_2 N_2)/A_0$. This surface occupancy has been shown [11] to vary among adaptations, since LLIMs have a greater occupancy ($p \approx 0.85$) than HLIMs ($p \approx 0.75$) due to paracrystalline domains. The mean number of open RCs in the stationary state is $N_o = N_1 - \frac{\lambda_C \gamma_A}{2(\gamma_D + \lambda_C)}\tau = N_1 - W\tau$. The linear $\lambda_C(N_o)$ assumption gives $\lambda_C(s, W) = \lambda_C^0(s) \times (1 - \frac{W\tau(s)(A_2 s + A_1)}{A_0 p(s)})$. The RC cycling time $\tau(s)$ is expected to vary somewhat with adaptations due to quinone diffusion and different metabolic demands, and is described with a linear interpolation using the values highlighted by arrows in Fig. 2(a). Likewise the rate $\lambda_C^0(s)$ must be zero when no RCs are present ($s \to \infty$), and takes a given value $\langle t_0 \rangle^{-1}$ when the membrane comprises only LH1s ($s = 0$). Its dependence on $s$ is satisfied by the form $\lambda_C^0(s) = (s/a + \langle t_0 \rangle)^{-1}$, with adjustable parameter $a$, for several computer generated membranes [see Fig. 4(c)]. Solving Eqs. (1) and (2) in the steady state, we obtain $W = \frac{\lambda_C(s,W)\gamma_A(s,I)}{2(\lambda_C(s,W)+\gamma_D)}$ which can be solved to yield

$$2W(s, I) = \frac{\gamma_A(s, I)}{2} + \frac{1}{B(s)}\left(1 + \frac{\gamma_D}{\lambda_c^0}\right) + \sqrt{\left[\frac{\gamma_A(s, I)}{2} + \frac{1}{B(s)}\left(1 + \frac{\gamma_D}{\lambda_c^0}\right)\right]^2 + \frac{\gamma_A(s, I)}{2B(s)}}, \quad (4)$$

where $B(s) = \frac{\tau(s)(A_1 + sA_2)}{p(s)A_0}$. As can be seen in Fig. 4(d) in the high stoichiometry or high intensity regime, too many excitations would dangerously increase the cytoplasmic pH [1,3,4]. Longer cycling times at higher light intensities are therefore helpful in order to keep power output bounded. The contours in Fig. 4(d) of constant quinol production rate $W$, show that only in a very small intensity range will bacteria adopt stoichiometries which are different from those experimentally observed in *Rhodospirillum photometricum* ($s \approx 4$ and $s \approx 8$) [10]. The empirical finding in Ref. [10] that membranes with $s = 6$ or $s = 2$ are not observed, is consistent with our theory. More generally, our results predict a great sensitivity of stoichiometry ratios for 30–40 $W/m^2$, below which membranes rapidly build up the number of antenna LH2 complexes. This prediction awaits future experimental verification.

In summary, our analytic and numerical calculations elucidate and quantify the interplay which arises between local (RC cycling) and extended dynamics (excitation transfer) in a chromatophore light-harvesting vesicle. In addition to explaining structural differences during growth, this new quantitative understanding may help accelerate development of novel solar micropanels mimicking natural designs.

F. C.-S. acknowledges financial support from Research Project Funds of Facultad de Ciencias, Universidad de Los Andes, and Fundación Mazda. We are grateful to S. Scheuring and J. Sturgis for detailed discussions. N. F. J. acknowledges F. Fassioli and A. Olaya-Castro for initial discussions.

[1] H. van Amerongen, L. Valkunas, and R. van Grondelle, *Photosynthetic Excitons* (World Scientific Publishing Co., Singapore, 2000).
[2] R. J. Sension, Nature (London) **446**, 740 (2007).
[3] T. Geyer and V. Helms, Biophys. J. **91**, 927 (2006).
[4] X. Hu *et al.*, Q. Rev. Biophys. **35**, 1 (2002).
[5] Y.-C. Cheng and G. R. Fleming, Annu. Rev. Phys. Chem. **60**, 241 (2009).
[6] S. Jang, M. D. Newton, and R. J. Silbey, Phys. Rev. Lett. **92**, 218301 (2004).
[7] M. Mohseni *et al.*, J. Chem. Phys. **129**, 174106 (2008).
[8] T. Ritz, S. Park, and K. Schulten, J. Phys. Chem. B **105**, 8259 (2001).
[9] H. Sumi, J. Phys. Chem. B **103**, 252 (1999).
[10] S. Scheuring and J. Sturgis, Science **309**, 484 (2005).
[11] S. Scheuring and J. Sturgis, Biophys. J. **91**, 3707 (2006); F. Fassioli *et al.*, Biophys. J. **97**, 2464 (2009).
[12] S. Bahatyrova *et al.*, Nature (London) **430**, 1058 (2004).
[13] S. Scheuring, J. Busselez, and D. Levi, J. Biol. Chem. **280**, 1426 (2004).
[14] S. Scheuring *et al.*, J. Mol. Biol. **358**, 83 (2006).
[15] R. P. Goncalves *et al.*, J. Struct. Biol. **152**, 221 (2005).
[16] T. Brixner *et al.*, Nature (London) **434**, 625 (2005); G. S. Engel *et al.*, Nature (London) **446**, 782 (2007).
[17] R. Agarwal *et al.*, J. Phys. Chem. A **106**, 7573 (2002).
[18] O. Savoth and P. Maroti, Biophys. J. **73**, 972 (1997).
[19] F. Milano *et al.*, Eur. J. Biochem. **270**, 4595 (2003).
[20] F. Caycedo-Soler, Ph.D. thesis, Universidad de los Andes, 2010, http://fimaco.uniandes.edu.co/investigacioni.html.